Demonstration of Adaptable Quality Radio System for Broadcasting of Speech

Martin Lima and Fredrik Esp Feyling

***Abstract*—This paper is presenting the design and implementation of a radio communication system for broadcasting of speech with adaptable data rate. This system is to be seen as a "proof of concept", where the main goal is to demonstrate a radio system with feedback from receiver (RX) to transmitter (TX) such that the transmitted data rate adapts to the state of the radio channel. The data rate is varied by a factor 2 by switching between QPSK and QAM-16 modulation while bandwidth and transmit power are fixed. The proposed system is implemented with a −55 dBc bandwidth of 220.6 kHz and a transmit power of −10 dBm.**

The adaptive quality feature is verified and the system changes quality immediately when the detected error rate drops below a predefined threshold. The measured bit error rates are $6.0 \cdot 10^{-2}$ and $1.4 \cdot 10^{-5}$ for high and low data rates respectively. The total delay from transmitter to receiver is measured to 262 ms, making the system well suited the for two-way communication as well as broadcasting.

I. Introduction

When designing any radio communication system, trade-offs has to be made between bandwidth, power, system complexity and bit rate. For a given bandwidth and transmit power, the bit rate could be varied by using different modulation schemes. As higher order modulation schemes require higher E_b/N_0, choosing optimum modulation scheme would require knowledge about the radio channel in order to maintain low enough BER at the receiver. This knowledge may be obtained by adding complexity in form of a feedback channel from receiver to transmitter. By performing some kind of error detection, the receiver may send information about detected error rates back to the transmitter. This enables the system to adapt the data rate to the state of the radio channel and thus provide better QoS for given power and bandwidth.

In this paper, we present a radio communication system with this kind of feedback structure. The system is to be seen as a "proof of concept", and the goal is not to propose a complete radio system for commercial use. The adaptable quality is obtained by implementing a feedback path from the receiver to the transmitter using frequency-division duplexing (FDD). In this demonstration, we simulate the varying state of the radio channel by changing the transmit power for a more controllable and reproducible test environment.

Figure 1 shows a top level block diagram of the proposed system. The figure shows that speech data is sent in the forward path from transmitter to receiver and the number of detected errors is sent in the feedback path from receiver to transmitter. The forward and feedback paths will be referred to as the *data path* and the *BER path* respectively. .

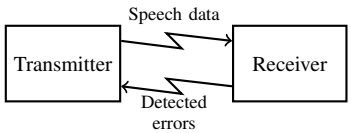

Fig. 1. Top level block diagram of proposed system. Speech data is sent in the forward path from transmitter to receiver and the number of detected errors is sent back from receiver to transmitter.

The proposed system is designed to switch between two different data rates, using two different modulation formats. Figure 2 shows a qualitative illustration of the adaptive quality concept. The proposed system may be further improved by adding more levels, yielding even better utilization of available resources.

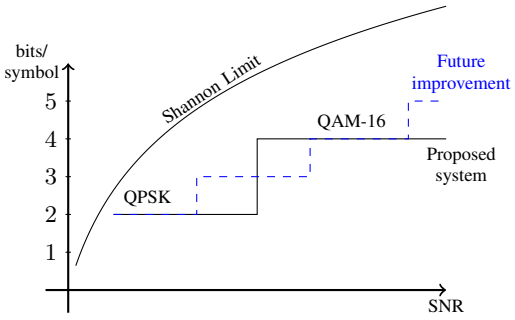

Fig. 2. Qualitative illustration of the adaptive quality concept

Throughout this paper, we will use the word *transmitter* when referring to the radio module that is transmitting the speech data and *receiver* when referring to the module that is receiving it. This is not to be confused with the terms TX and RX, which we use when referring to the transmit and receive port on each radio module.

The system is implemented using the software defined radio USRP-2901 [1] from National Instruments which contains all necessary RF hardware. All the software parts of the system is implementing in C++ and is executed on a standard personal computer. Pre-written C-libraries are used for the parts of the system concerning interface to the USRP, the computer sound card etc. These parts will not be explained in detail, but references to the libraries will be given. For the remaining parts of the system, we focus on explaining the implementation on a behavioural level and detailed descriptions of C code implementations is avoided.

In section II, we present the system specifications and the link budget is presented in section III together with associated measurements. A detailed description of the proposed system is given in section IV and the motivation behind some crucial design decisions is presented in section V. Performed measurements is presented in section VI before a final conclusion is given in section VII.

II. System Specifications

The proposed radio communication system is designed to switch between QPSK and QAM-16 modulation in order to obtain adaptable sound quality. The system use the 2.4 GHz ISM band with a carrier frequency of 2.415 GHz and 2.455 GHz for the data path and BER path respectively. The system is designed for a transmission distance of 5 meter in an indoor environment.

Some key system specifications are listed in table I and II. Table I shows the parameters for the data path, for low / high data rate transmission. Table II shows parameters for the simpler BER path.

The burst format for the transmitted data is shown in figure 3.

TABLE I
SYSTEM SPECIFICATIONS - DATA PATH

System Variables	Value Low / High Data rate
Frequency f_0	2415 MHz
Modulation	QPSK/QAM-16
Sound sampling rate f_s	11025/22050 Hz
Bits per sound sample b_s	12 bits
Sound datarate R_{ss}	132/265 kbits/s
Channel coding	Hamming (4,7)
Packet Parameters	
Packet header size	8 bits
Packet size	512 bits
Frame Parameters	
Training sequence type	Barker
Training sequence length	26 symbols
Burst Parameters	
Guard period	2 symbols
Burst Length	484/256 symbols
Transmission Characteristics	
Symbol rate R_s	150 ksymbols/s
Samples per Symbol	8
Pulse shaping filter	root raised cosine
Pulse shaping filter parameter α	0.5
Minimum Nyquist bandwidth Δf	112.5 kHz

TABLE II
SYSTEM SPECIFICATIONS - BER PATH

System Variables	Value Low / High Data rate
Frequency f_0	2455 MHz
Modulation	QPSK
Channel coding	Hamming (4,7)
Packet Parameters	
Packet header size	8 bits
Packet size	26 bits
Frame Parameters	
Training sequence type	Barker
Training sequence length	26 symbols
Burst Parameters	
Burst Length	43 symbols
Transmission Characteristics	
Symbol rate R_s	150 ksymbols/s
Samples per Symbol	8
Pulse shaping filter	root raised cosine
Pulse shaping filter parameter α	0.5
Minimum Nyquist bandwidth Δf	112.5 kHz

The bursts are different when using QPSK and QAM-16 modulation because the same number of training symbols maps to a different number of bits. The data packets (a and b) are transmitted continuously with the indicated guard period. The BER packets are very small compared to the data packets and are only transmitted once per received data packet. Thus no guard period is specified for these packets.

Note that this system is implemented with constant payload size which means that the packet rate is varied when the data rate changes.

III. LINK BUDGET

The link budget for the system is shown in table III. The system is designed to operate indoors with a distance of 5 meters between transmitter and receiver. Table III shows losses from propagation, loss in TX and RX, and some estimated key parameters at the receiver.

In this demonstration, the transmit power is varied in order to simulate changes in the radio channel while the physical radio link is fixed. Hence no fading statistics is included in the link budget. The stated values are based on the transmit power used for high data rate transmission corresponding to the best simulated state of the radio channel.

Training sequence 52	Session ID 3	Packet ID 5	Payload 512	Guard bits 4

(a) QPSK data packet

Training sequence 104	Session ID 3	Packet ID 5	Payload 512	Guard bits 8

(b) QAM-16 data packet

Training sequence 52	Session ID 3	Packet ID 5	Payload 26

(c) QPSK BER packet

Fig. 3. Burst format (bits) for QPSK(a) and QAM-16(b) modulated data packets, and QPSK modulated BER packet (c)

TABLE III
LINK BUDGET

TX Loss	Value Low / High Data rate
PA Power, P_{PA}	−10 dBm
TX Connector Loss, L_{ConT}	−0.3 dB
TX Power, P_T	−10.6 dBm
TX Antenna Gain, G_T	1.5 dBi
Effective (Isotropic) Radiated Power, EIRP	−9.1 dBm
Path Loss	
Distance, d	5 m
Floor loss factor, $P_f(n)$	0 dB
Distance power loss coefficient, N	38
Total ITU path loss, L_P	−66.22 dB
RX Loss	
RX antenna gain, G_R	1.5 dBi
RX connector loss, L_{ConR}	−0.3 dB
Total RX Loss, L_R	0.9 dB
RX Loss	
Total Received Power, P_R	−74.42 dBm
Antenna Noise Density, N_0	−145.73 dBm/Hz
Antenna Total Noise Power, N	−92.72 dBm
RX Noise Figure, NF	7.0 dB
RX Properties	
Carrier-to-noise ratio, C/N	11.3 dB
Eb over N0, E_b/N_0	9.54 dB /6.23 dB

The value for connector loss is taken from the data sheet of a standard coaxial RF connector [2]. The antenna gain value is taken from the data sheet [3].The transmit power, P_{PA}, was adjusted after measurements to obtain appropriate $^{E_b}/_{N_0}$ at the receiver.

The estimated path loss constitutes solely of the propagation loss obtained from the ITU Indoor Propagations Loss Model [4]. The loss model consists of two adjustable factors, the distance power loss coefficient, N, and the floor loss penetration factor, $P_f(n)$. The latter is set to 0, and the former was set to 38 after calibrating the test environment. Figure 4 shows the measured path loss and the prediction from the ITU model before and after adjusting the power loss coefficient.

Other loss factors such as pointing loss and polarisation loss was considered, but measurements showed that the amount of reflections in the room made pointing and polarisation irrelevant to the received power.

The antenna noise density was measured with a spectrum analyser and the estimated value was taken as an average of several single runs. The noise figure of the receiver is included to account for noise added by the radio hardware, with value taken from the data sheet.

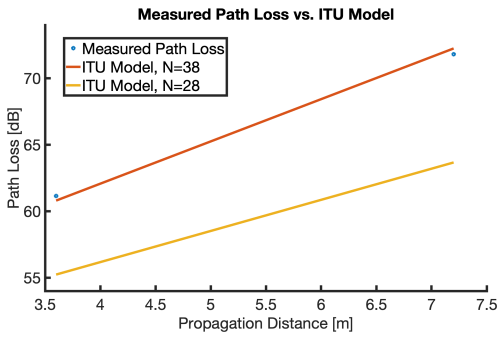

Fig. 4. Measured path loss vs. estimated path loss from the ITU Indoor Propagations Loss Model, before and after adjusting the power loss coefficient

IV. Design Description

Figure 1 shows how the transmitter and receiver communicates within the system. Block diagrams for the two subsystems are shown in appendix A, figure 13 and 14. The data rate between each block of the data path is indicated with the thin arrows. The behavior of the system will be explained in this section.

Because two different modulation schemes are used, the receiver need to know how to decode the incoming data packets. This problem is solved by using two different training sequences in the beginning of each frame. As shown in figure 13, the receiver performs a check on the received Barker sequence before de-mapping the symbols.

In the transmitter, *Session State* keep the information about what data quality and modulation scheme to use. As figure 13 indicates, the session state influences several blocks of the TX side of the transmitter. The decision of when to change data quality is left to the transmitter. For every received data packet, the receiver computes the number of detected errors and transmit this number back to the transmitter. These BER packets are always transmitted using QPSK-modulation. Based on the received number of detected errors, the transmitter decides whether to change session state or not.

The sound producer and sound consumer contain functionality for handling the sound input and output to the sound card of the computer. They are implemented using the Windows API [5]. Sound producer reads sound samples from the sound card at full quality (16 bit, 44100 Hz stereo) and writes the samples to a queue accessible for the source encoder. Sound consumer equivalently reads sound samples from a queue controlled by the sound decoder block and writes to the computer sound card.

The source encoder performs lossy compression of the produced sound samples. The bit resolution is reduced to 12 bit, and the sampling rate is reduced by a factor 2 or 4 depending on the session state. The source decoder performs the inverse operation, by upsampling with a factor of 2 or 4.

In the packing block, sound data is read from the source encoder, a header is added, and the packet is sent to the packet queue. The eight bit packet header consists of a three bit session ID and a five bit packet ID.

A scrambler is implemented before FEC which computes a bitwise XOR between a pseudo random bit string and the packet. The bit string used for scrambling is of the same size as the packet itself. The scrambler performs the exact same operation at RX and TX.

The implemented FEC algorithm is Hamming (7,4). The C-implementation uses fast table lookups, written by Michael Dipperstein [6].

The system uses Grey Code for mapping the binary data to a complex vector z. The mapping schemes are shown in figure 5.

```
%====QPSK=====%
%=============%
%   Coding    %
%  01   |  00  %
% ----------- %
%  11   |  10  %
%=============%
```

(a)

```
%============16QAM=============%
%================================%
%            Coding              %
%   0000  0100 | 1100  1000     %
%              |                 %
%   0001  0101 | 1101  1001     %
%  --------------------------    %
%   0011  0111 | 1111  1011     %
%              |                 %
%   0010  0110 | 1110  1010     %
%================================%
```

(b)

Fig. 5. Symbol mapping for QPSK (a) and QAM-16 (b) modulated symbols

The training sequence is added to both I and Q symbols in the block *Add Barker*. The training sequence is an appropriate repetition of Barker sequences of length 7 and 13 for QPSK and QAM-16 modulation respectively. The total length of the training sequence is 26 symbols.

In the last step before transmission, the symbols are upsampled by a factor 8 and filtered with a pulse shaping filter. The filter is a Root Raised Cosine with a roll-off factor of 0.5. The same filter is applied as a matched filter in the first step at the receive side before the samples are downsampled again.

The USRP is configured to transmit continuously with a symbol rate of 150 symbols per second and transmits I/Q zeros when no data is available. A 100 ms USB buffer is used on both TX and RX side of the USRP to minimize the effects of USB-latency. The USRP interface is implemented using the NI-USRP DLL [7].

Symbol synchronization is done by choosing the sample offset that maximizes the signal energy.

Frame synchronization is done by computing the crosscorrelation between the two training sequences and the received symbols. After a frame is found, only the frame symbols are passed along to the next block.

A. Frequency and Phase Synchronization

The implemented frequency synchronization algorithm is based on the Mth-power algorithm [8], which is further improved by using a Kalman filter. Frequency offset is estimated from the training sequence only. The Mth-power algorithm estimates the phase offset of MPSK modulated symbols by mapping all symbols to the same point in the complex plane. By tracking the angular difference between consecutive symbols, the frequency offset may be estimated. In our case, the QPSK symbols of the training sequence is raised to the 4th power, and the phase is estimated as indicated in figure 6.

For each received frame, the frequency offset is estimated by the mean of the angular difference between all consecutive symbols of the training sequence. The accuracy of the estimate is improved by the use of a Kalman filter.

After frequency correction, the phase offset is estimated as the mean of the angular deviation between the training sequence of the received symbols and the ideal Barker sequence.

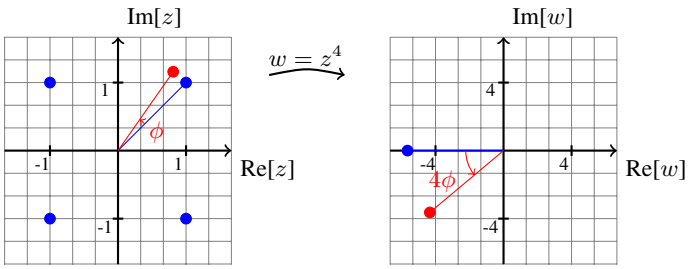

Fig. 6. Illustration the mapping $w = z^4$ which indicates how a phase error in QPSK modulated signal can be observed.

V. Design Motivation

The goal of the proposed system is to demonstrate a radio communication system with adaptable sound quality. This main goal is the background for all design choices that is made. In this section, the motivation behind the key specifications and some of the solutions described in section IV is given.

A. System specifications

1) Transmit Power: As shown in table III, the transmitter PA power, P_{PA}, is set to -10 dBm. As the purpose of the system is to demonstrate the adaptable quality feature, the transmit power was tuned to a value suitable for this purpose. Too high transmit power would give a received E_b/N_0 high enough to always transmit at the best quality, thus disabling us from demonstrating the quality adoption.

2) Modulation Scheme: The system uses QPSK for low data rate transmission and QAM-16 for high data rate transmission. QPSK has the advantage of constant symbol amplitude and therefore reduces nonlinear effects in the amplifiers. Because of the orthogonality between the I and Q signals, QPSK also gives twice the capacity as BPSK for same E_b/N_0 sensitivity. QAM-16 is chosen for high data ratenrs because the information content in each symbol is twice as big as for QPSK, making the difference big enough to demonstrate an audible effect.

3) Bandwidth: The motivation behind the adaptable quality feature, is to maximise data rate, for fixed bandwidth and transmit power. To demonstrate this feature, the system is designed width a fixed bandwidth, equal for both quality levels. The specific value for the bandwidth is however not important for this demonstration. The transmitted symbol rate is chosen large enough to enable both QPSK and QAM-16 transmission. The ideal Nyquist bandwidth is calculated from the symbol rate and the properties of the pulse shaping filter, and presented in table III.

B. System Architecture

The adaptable quality feature requires some additional logic, compared to a system without a feedback path. One important design choice is to determine where the decision of changing quality level (referred to as *state*) is to be made. During the design of the proposed system, two solutions were considered:

1) The receiver decides when to change state and sends a simple message to the transmitter, telling it to change state. The receiver has its own state variable, and updates it after sending the message to the transmitter.
   The advantage of this solution is that the receiver always know how the received symbols are modulated. Thus, no state information is needed in the transmitted packet.
   The draw back is that there will be some delay from the receiver ask for a change of state, until state change is completed. This will either cause a few packets to get lost in the meantime, or extra logic must be implemented to handle the issue. Extra logic must also be implemented to handle the case of bit errors in the "change-state-message".
2) The transmitter decides when to change state and the receiver continuously send information about detected error rate to the transmitter. This requires information about the state to be contained in the data packet and the receiver will need more complexity in order to determine the incoming modulation format. However, this will eliminate the risk of having the transmitter and the receiver are in different states.

We chose to implement the second solution. The state information is kept in the two different Barker sequences. Because we would have to search for one Barker sequence in the frame synchronization anyway, searching for one more would be both computationally fast and easy to implement. In addition, the good autocorrelation properties of the Barker sequence makes the state information robust against noise, and no extra FEC is needed to keep this information safe.

C. Implemented Functionality

1) Source Encoding: We chose not to implement any source encoding except for the primitive reduction of data rate. A source encoder removes redundancy in the speech data and increase the information content of every transmitted symbol. This functionality is not necessary to demonstrate the adaptable quality and is therefore not implemented.

The source encoder also makes the system more sensitive to bit errors, as the information content in each bit is increased. Our system is designed to operate at E_b/N_0 low enough to demonstrate the quality adaption. When the received E_b/N_0 falls low enough to make the system change from QAM-16 to QPSK modulation, we would like the system to have a large margin before the BER for QPSK also get too high and the link is broken. Using a source encoder would make this window smaller and the system would be harder to demonstrate.

2) Scrambler: Analysis of the received constellation diagram clearly showed that some symbols occurred more frequently at the receiver than others. Both the RF hardware and the pulse align algorithm are highly sensitive unequal energy distribution between I and Q. When comparing the received constellation from speech data to the constellation from random data, we could see that the quality was considerably increased when transmitting white data. We therefore implemented a scrambler to whiten the speech data before transmission.

3) FEC: The implemented FEC algorithm is Hamming(7,4) and serves two purposes. In the data path, the receiver must estimate the number of bit errors and send this number back to the transmitter. In the BER path, the transmitter use the FEC to determine the validity of the received BER packet. If the number of bit errors in the BER packet is above a predefined threshold, the packet is discarded in order to reduce the risk of undesired changes of quality level.

This particular algorithm was chosen for its simplicity and decent trade-off between redundancy overhead and minimal Hamming distance. Detection of any two-bit errors in every 7 bit code word was considered sufficient for this purpose. In addition, a pre-written implementation exists [6] which saved development time.

4) Frequency and Phase Synchronization: The Mth-power algorithm is chosen for frequency synchronization because of the good accuracy and simple implementation. By estimating the frequency offset as the mean of the angular deviation between all consecutive symbols, the ML estimate of the frequency offset is obtained. In

addition, the Mth-power algorithm does not require a known training sequence, and may be applied to all data samples when QPSK modulation is being used. By extending the algorithm to a Kalman filter, the mean square error between the estimated offset and the actual offset is minimized. The improvement from the Kalman filter is clearly seen in figure 7 which shows the estimated frequency offset at the receiver with and without Kalman filter.

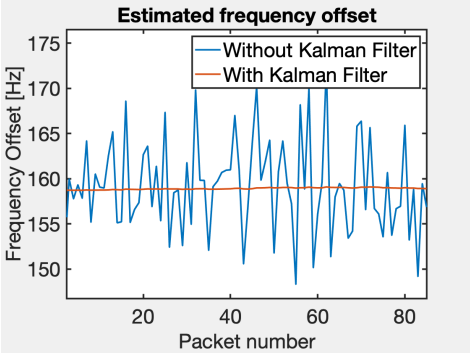

Fig. 7. Estimated frequency offset with and without Kalman filter

The Mth-power algorithm is however not linear, making it less suited for phase estimation. Therefore, the linear algorithm based on comparing the phase directly to the training sequence is used for estimating the phase.

VI. Measurements and Verification

In this section, we present measurements and verifications of the proposed system. We first present a verification of the system specifications in section VI-A. In section VI-B the system performance will be evaluated under different conditions, and some key performance parameters will be presented.

A. Verification of System Parameters

The verified system specifications are summarized in table IV.

TABLE IV
Summarised Measurements of System Parameters

System Parameter	Measured Value
Half-Power Bandwidth	220.6 kHz
PA power, P_{PA}	−10 dBm
Delay	262 ms

The power spectrum of the signal was analyzed in MATLAB's signal analyzer toolbox [9]. The baseband power spectrum is shown in figure 8 together with the theoretical spectrum. A −55 dBc bandwidth was chosen as the power outside this region is negligible. The bandwidth was measured to be 220.6 kHz. The transmit power was verified by first calibrating the USRP power spectral density using a spectrum analyzer, and then calculating the total transmit power from measured bandwidth[1]. This way, the transmit power was measured to −10 dBm.

The system delay was measured by transmitting timestamps and evaluating the time delay from sound producer to sound consumer. The delay was measured by running both the transmitter and receiver software on the same computer. The average measured delay was 262 ms with a sample standard deviation of 63 ms. 200 ms of this delay originates from the buffers of the USRP.

[1]Due to the COVID-19 situation, the lab equipment was not available for measurements on the implemented system

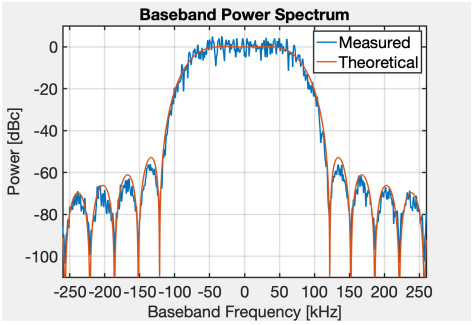

Fig. 8. Received signal power spectrum

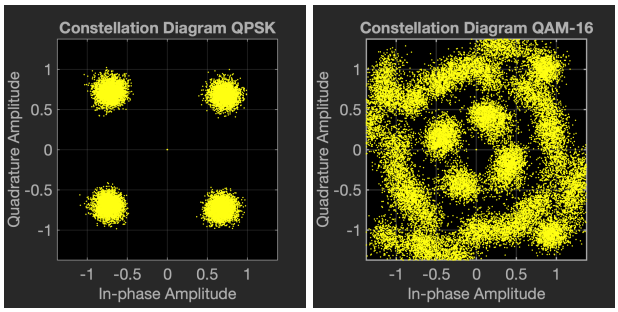

(a) QPSK constellation (b) QAM-16 constellation

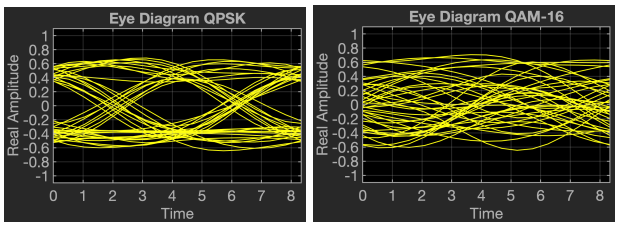

(c) QPSK eye diagram (d) QAM-16 eye diagram

Fig. 9. Eye diagram and constellation for QPSK (a and c) and QAM-16 (b and d) modulated symbols. Transmit power: −10 dBm

B. Performance Measurements

The system is tested in an indoor environment with both USRP's at the same height, 1 meter apart and no polarization mismatch[2]. For the sake of reproducibility, we chose to simulate the varying state of the radio channel by adjusting the transmit power instead of changing the radio channel physically. Two different transmit power levels was used to verify transmission at both qualities. High quality transmission was measured with a transmit power of −10 dBm and low quality with −25 dBm.

Eye diagram and constellation diagram are provided for both transmit power levels and both modulation formats, together with some key performance measurements. The diagrams for high and low transmit power are summarized in figure 9 and 10 respectively. Estimated performance parameters are summarized in table V and VI for high and low transmit power respectively. In these tables, BER is the true measured bit error rate, while the error vector magnitude (EVM) and SNR are estimated from the constellation diagrams by comparing ideal and received constellations. E_b/N_0 is estimated using the measured −55 dBc bandwidth for noise power.

[2]The measurements had to be performed in a tiny student apartment because the lab was closed down.

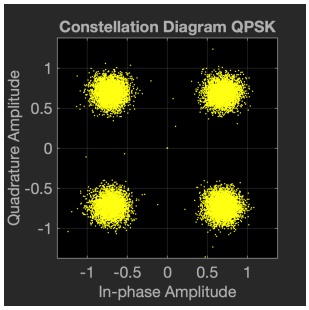

(a) QPSK constellation

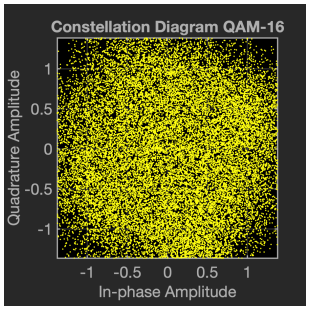

(b) QAM-16 constellation

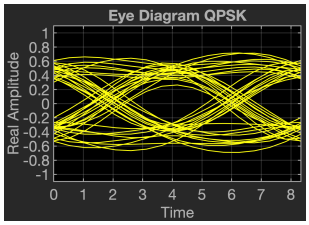

(c) QPSK eye diagram

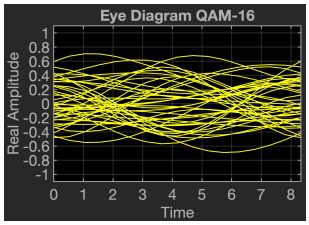

(d) QAM-16 eye diagram

Fig. 10. Eye diagram and constellation for QPSK (a and c) and QAM-16 (b and d) modulated symbols. Transmit power: $-25\,\mathrm{dBm}$

TABLE V
MEASURED PERFORMANCE PARAMETERS. TRANSMIT POWER: $-10\,\mathrm{dBm}$

System Parameter	Measured Value Modulation QPSK / QAM-16
SNR	$18.1\,\mathrm{dB}/12.8\,\mathrm{dB}$
E_b/N_0	$13.1\,\mathrm{dB}/4.6\,\mathrm{dB}$
BER	$1.35 \cdot 10^{-6}$ / $6.0 \cdot 10^{-2}$
EVM	$-17.5\,\mathrm{dB}/-14.5\,\mathrm{dB}$

Figure 11 shows the measured BER as a function of estimated E_b/N_0. This value is compared to a theoretical BER (Estimated BER) to give an impression of the system performance under the given conditions. The BER is measured with 10^4 frames of 1150 bits each, making $8.7 \cdot 10^{-8}$ the smallest detectable BER. The estimated BER is based on white Gaussian noise only.

C. Discussion of Obtained Results

The proposed system is supposed to broadcast speech data with adaptable sound quality, by switching between QPSK and QAM-16 modulation based on the detected error rates. During the full system test, the threshold for changing state was set to $1 \cdot 10^{-2}$. With this threshold, the system changed quality state when the transmit power was reduced to about $-17\,\mathrm{dBm}$. The test verified that the adaptable quality feature works as expected. The measured 262 ms delay show that the system is well suited for two-way communication as well as broadcasting.

TABLE VI
MEASURED PERFORMANCE PARAMETERS. TRANSMIT POWER: $-25\,\mathrm{dBm}$

System Parameter	Measured Value Modulation QPSK / QAM-16
SNR	$15.9\,\mathrm{dB}/10.16\,\mathrm{dB}$
E_b/N_0	$11.9\,\mathrm{dB}/3.8\,\mathrm{dB}$
BER	$1.4 \cdot 10^{-5}$ / $1.32 \cdot 10^{-1}$
EVM	$-16.1\,\mathrm{dB}/-12.8\,\mathrm{dB}$

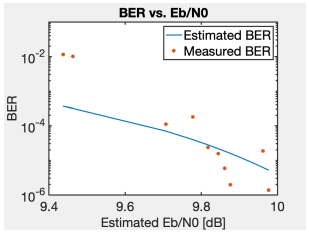

(a) QPSK

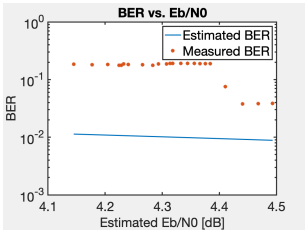

(b) QAM-16

Fig. 11. BER vs. SNR for both modulation formats. The estimated BER is the theoretical BER based on the estimated values for $E_b/N_0$and true BER is the actual calculated BER

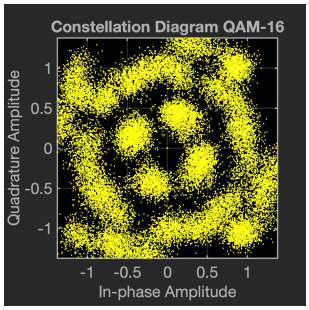

(a) Full frame

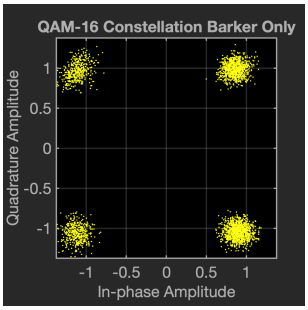

(b) Barker only

Fig. 12. QAM-16 constellation with full frame and Barker symbols only. Transmit power: $-10\mathrm{dBm}$

Figure 8 shows that the measured power spectrum lies very close to the theoretical spectrum. This indicates that the amount of nonlinear distortion introduced by the RF hardware is at a minimum.

When transmitting QPSK modulated data at low data rate, the system delivered almost noise free sound, at both power levels. The sound quality was not audibly reduced by the transmission. Figure 9 and 10 and table V and VI supports this qualitative description.

The transmission of QAM-16 modulated data was not equally successful. At the highest power level, the transmitted speech was highly influenced by noise. At the lowest power level, the speech and noise could not be differentiated. This result is again supported by figure 9 and 10, and table V and VI. The constellation diagram in figure 9 (b) shows that the poor quality is mainly due to bad phase synchronization. Figure 12 shows a comparison of the QAM-16 constellation with all frame symbols (a), and with the Barker symbols only (b). As the figure shows, the Barker symbols have no visible phase shift, which indicates that there is a phase difference between the Barker symbols and the rest of the frame. The reason for this problem is not understood by the authors and the issue remains for future improvements.

The BER vs. E_b/N_0 plots of figure 11 gives an indication of how well the system performs under the given noise conditions, by comparing the measured BER to estimated BER, assuming white Gaussian noise only. For the QPSK modulated signal, the measured BER is higher than estimated for low E_b/N_0, and approaches the theoretical value as E_b/N_0increase. This is because the frequency and phase synchronization algorithms get less accurate as the noise level increase, which introduces more errors than what is obtained from AWGN only. For the QAM-16 modulation, the BER is constantly above the theoretical value, mostly because of the poor phase synchronization discussed previously.

VII. Conclusion

The design and implementation of a radio communication system for broadcasting of speech with adaptable data rate is presented. The system adapts the transmitted data rate to the state of the radio channel by evaluating detected bit error at the receiver. The transmitted data rate is varied by a factor 2 by switching modulation format between QPSK and QAM-16.

The system was verified in an indoor environment with a transmission distance of 1 meter and variations in the radio channel is simulated by adjusting the transmit power. The system transmit at high data rate (520.8 kb/s) when using QAM-16 modulated symbols at -10 dBm and low data rate (249 kb/s) for QPSK at -25 dBm. Bit error rates of $6.0 \cdot 10^{-2}$ and $1.4 \cdot 10^{-5}$ was measured at high and low data rate respectively.

The high BER for QAM-16 modulation makes the effect of adaptable quality hardly audible because of the high noise level when transmitting at high data rate. The adaptable quality feature is however interesting in itself and this demonstration shows a working "proof of concept". By adapting the transmitted data rate to the state of the radio channel, the system yields a better utilization of available resources. This two-level adaption could be extended to several levels for higher performance in future improvements.

References

[1] National Instruments, "Usrp-2901 specifications - national instruments," https://www.ni.com/pdf/manuals/374925c.pdf, (Accessed on 04/16/2020).

[2] TE Connectivity, "Rf coaxial connectors," https://www.mouser.com/datasheet/2/418/NG_DS_1-1773725-8_RF_COAX_QRG_0114_TE-1948_RFcoaxi-1232379.pdf, (Accessed on 04/14/2020).

[3] Siretta, "Delta-7a datasheet," https://docs.rs-online.com/a8a8/0900766b81540fe9.pdf, (Accessed on 04/14/2020).

[4] International Telecommunication Union, "Recommendation itu-r p.1238-10," https://www.itu.int/dms_pubrec/itu-r/rec/p/R-REC-P.1238-10-201908-I!!PDF-E.pdf, (Accessed on 04/14/2020).

[5] Microsoft Corporation, "Windows api index," https://docs.microsoft.com/en-us/windows/win32/apiindex/api-index-portal, (Accessed on 05/03/2020).

[6] M. Dipperstein, "Hamming (7,4) code discussion and implementation," http://michael.dipperstein.com/hamming/, (Accessed on 04/20/2020).

[7] National Instruments Corporation, "Labview nxg - national instruments," https://www.ni.com/en-no/shop/labview/labview-nxg.html, (Accessed on 05/03/2020).

[8] A. Viterbi, "Nonlinear estimation of psk-modulated carrier phase with application to burst digital transmission," *IEEE Transactions on Information Theory*, vol. 29, no. 4, pp. 543–551, 1983.

[9] MathWorks, "Using signal analyzer app - matlab," https://se.mathworks.com/help/signal/ug/using-signal-analyzer-app.html, (Accessed on 05/02/2020).

Appendix A
Block Diagram

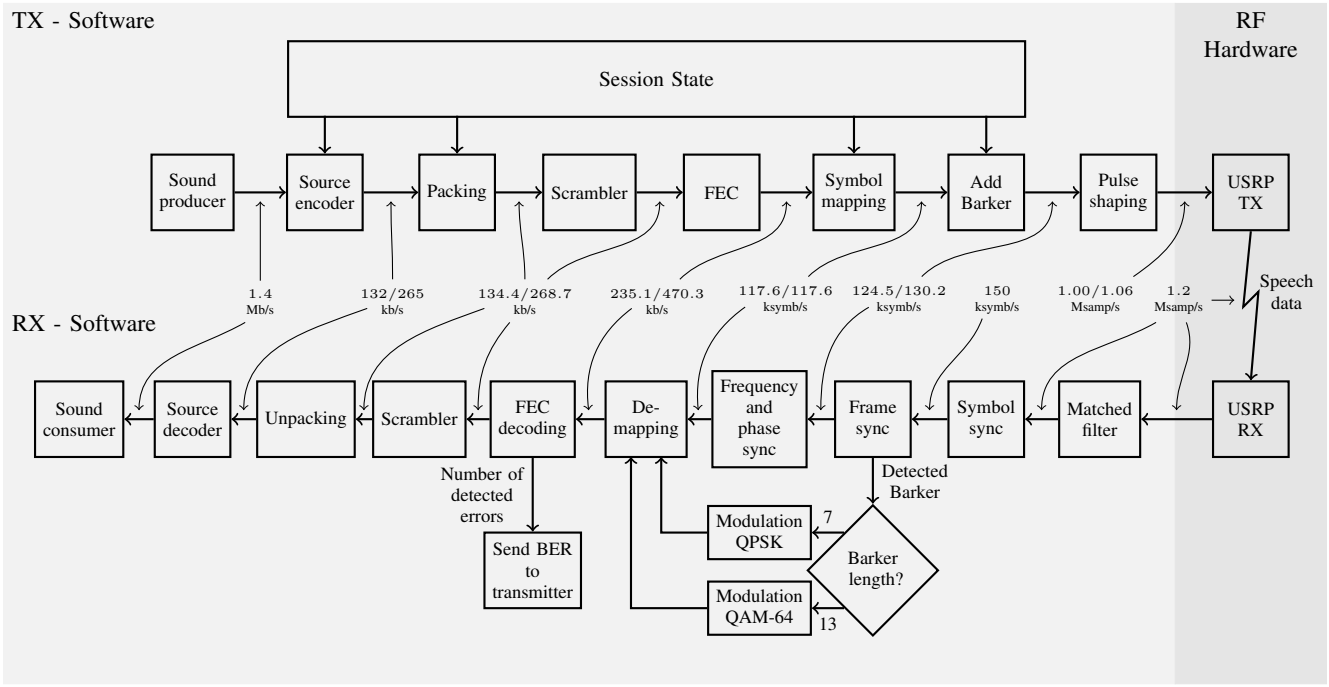

Fig. 13. Block diagram of data packet system. This block diagram shows the forward path of the system, where speech data is being transmitted. Data rates for Low/High data quality is indicated on each arrow.

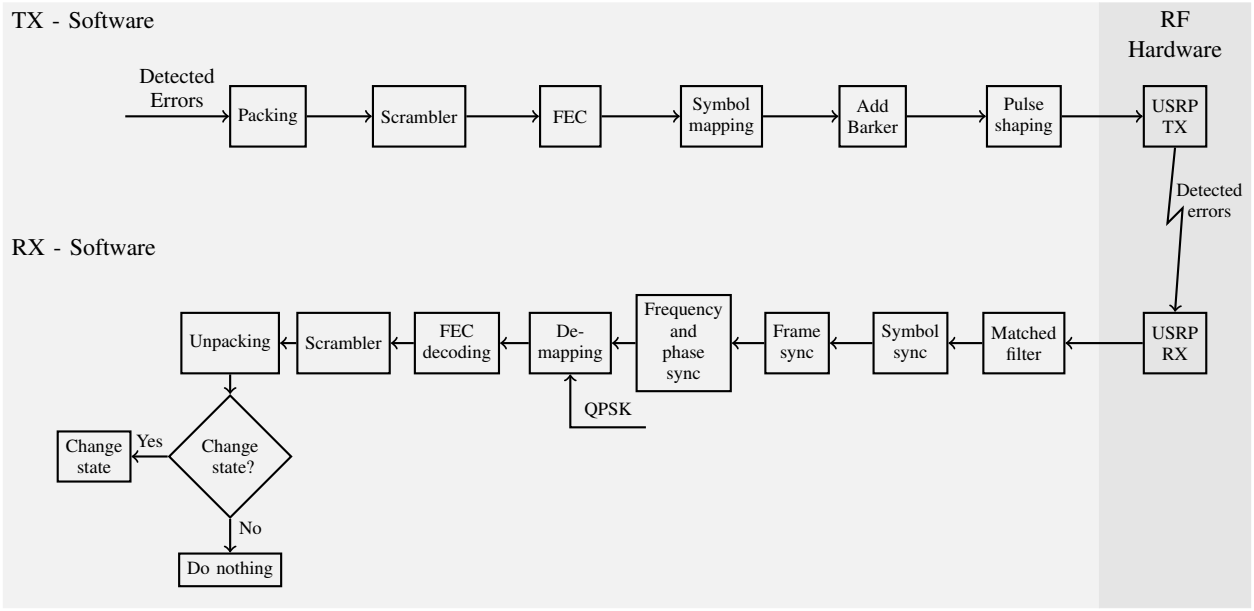

Fig. 14. Block diagram of BER packet system. This sub-system constitutes the feedback path where the receiver transmit information about detected error rate back to the transmitter.